Shape design of millimeter-scale air channels for enhancing heat transfer and reducing pressure drop

Chin-Hsiang Cheng [a,*], Chi-Kang Chan [b], Guang-Jer Lai [b]

[a] *Department of Aeronautics and Astronautics, National Cheng Kung University, No. 1, Ta Shieh Road, Tainan, Taiwan 701, ROC*
[b] *Department of Mechanical Engineering, Tatung University, No. 40, Chungshan N. Road, Sec. 3 Taipei, Taiwan 104, ROC*

Abstract

The present study is aimed at shape design of a millimeter-scale air channel for increasing heat transfer to the air from the heated channel wall and reducing pressure drop between the inlet and the outlet. The approach is developed by combining a direct problem solver with an optimization method. A two-dimensional theoretical model is used to develop a direct problem solver, which provides the numerical predictions of the thermal and flow fields associated with the varying shape profile during the iterative optimization process. Meanwhile, the simplified conjugate-gradient method (SCGM) is used as the optimization method which continuously updates the shape until the objective function is minimized. In this paper, a method based on a point-by-point technique for constructing the shape profile is employed. This method is particularly suitable for determining the irregular profiles that cannot be approximated by the polynomial functions. The optimal shapes at different inlet velocities are obtained. It is found that the search process is robust and always leads to the same optimal solution regardless of the initial guess.
© 2007 Elsevier Ltd. All rights reserved.

1. Introduction

Inverse methods are often used in heat transfer analysis to determine parameters which are difficult or impossible to measure directly, from carefully selected experimental measurements which can be more easily carried out. The development of the inverse heat transfer problems (IHTP) received considerable impetus from the space program starting from about 1956. A Russian paper presented by Shumakov [1] solving the heating process of a solid body by the IHTP approach was translated in 1957. Later, Stolz [2] dealt with the inverse heat conduction problem for calculating the heat transfer rates during quenching process from the objects with simple geometries. Nowadays, the IHTP approach has been used to determine the unknown boundary temperature [3], surface heat flux [4,5], internal heat generation [6], contact resistance [7], and thermal properties of the working mediums [8,9].

Likewise, the shape design problems are also regarded as an important kind of IHTP problems. Practical applications of the shape design problems include the optimization for the geometry of the power systems [10,11], the shape design of thermal and fluid units [12–17], and shape identification for unknown bodies [18]. In general, the problems raised in the practical shape design problems are normally to find an optimal geometry for a heat transfer system so as to increase the thermal performance or to meet some specific heat transfer requirements. Nowadays, there are a number of optimization methods available, such as the growth-strain method [19], the singular superposition method [20], the level set method [21], and the multi-objective optimization method [22], which can be used to yield the optimal designs for different devices.

---

* Corresponding author. Tel.: +886 6 2757575x63627; fax: +886 6 2389940.
E-mail address: chcheng@mail.ncku.edu.tw (C.-H. Cheng).

Nomenclature

a_i	undetermined coefficients to optimize
b_1, b_2	profile coefficients of shape function 1
c_1, c_2, c_3, c_4	profile coefficients of shape function 2
C_1, C_2	weighting factors
C_P	specific heat, 1.004 kJ/(kg K)
D	channel depth, m
$h(x)$	channel width function, m
h_i	inlet channel width, 1.8 mm
h_o	outlet channel width, m
$\bar{h}$	arithmetic average channel width
J	objective function
k	thermal conductivity, 2.5743×10^{-2} W/(m K)
L	length of channel, 10 mm
L_s	arc length of the designed adiabatic wall, m
N	outward normal coordinate to the designed wall surface
P	pressure, Pa
P_i	average inlet pressure, Pa
P_o	average outlet pressure, 0 Pa
Re	Reynolds number, $\rho V_i h_i / \mu$
T	air temperature, K

T_i	average inlet air temperature, 298 K
T_o	average outlet air temperature, K
T_H	heated wall temperature, 328 K
T_L	low temperature, 298 K
u	velocity in x-direction, m/s
v	velocity in y-direction, m/s
V_i	inlet velocity, m/s
$\vec{V}$	velocity vector, $u\vec{i} + v\vec{j}$
x, y, z	rectangular coordinates

Greek symbols

β	search step size
γ	conjugate gradient coefficient
μ	dynamic viscosity, 1.8135×10^{-5} N s/m^2
π	search direction
ρ	air density, 1.205 kg/m^3
τ	shear stress, kN/m^2

Superscript

n	iteration number

In recent years, heat transfer to a fluid in a small channel has received great attention in the heat transfer area as well as in industry. It is well known that the convective heat transfer coefficients are inversely proportional to the hydraulic diameter under laminar flow at a constant heat transfer rate; therefore, smaller channels are capable of providing higher heat transfer coefficients and hence greatly reducing the thermal resistance to the heat flow in the compact heat exchangers. Millimeter-scale channels, commonly having hydraulic diameters of 0.5–3 mm, are useful not just in the compact heat exchangers, but also in the electronic cooling systems and the fuel cells. Wambsganss et al. [23] performed two-phase flow experiments with air/water mixtures in a small rectangular channel measuring 9.52×1.59 mm for applications to compact heat exchangers. In this paper, pressure drop data are presented as a function of both mass quality and Martinelli parameter and are compared with the existing correlations. Lately, heat transfer and pressure drop for boiling water flow in a millimeter-scale circular copper channel of 0.706-mm diameter are measured by Campbell and Kandlikar [24]. Recently, Bahrami and Yovanovich [25] investigated the pressure drop of a fully-developed, laminar, incompressible flow in the smooth millimeter- and micrometer-scale channels of arbitrary cross-section is investigated. An approximate model is proposed that is used to predict the pressure drop for a wide variety of cross-section shapes.

Based on the existing information, it is recognized that a smaller channel leads to higher heat transfer rate; however, the pressure drop between the inlet and the outlet of the channel is also greatly increased. It is also found that the pressure drop is greatly dependent on the geometry of the channel. The pressure drop, representing the loss of pressure in a compressed air system due to friction or restriction, becomes severe particularly in the millimeter- and micrometer-scale channels. In general, a significant reduction in pressure drop without a remarkable loss in heat transfer is desired.

Therefore, design for the shape profile of the air channel for obtaining a lower pressure drop between the inlet and the outlet while still increasing the heat transfer to the air from the heated channel wall is attempted in the present study. The numerical design approach is developed by combining a direct problem solver with an optimization method. A two-dimensional theoretical model is used to develop the direct problem solver for predicting the thermal and flow fields associated with the varying shape profile during the iterative optimization process. On the other hand, the simplified conjugate gradient method (SCGM) is used as the optimization method. The SCGM method, proposed by Cheng and Chang [26], is capable of handling the objective functions defined in different forms, and thus it widens the flexibility of the application of the optimization method. In the SCGM method, the sensitivity of the objective function to the designed variables is firstly evaluated, and then by giving an appropriate fixed value for the step size, the optimal design can then be carried out without overwhelming mathematical derivation. Lately, this method was successfully employed by the same group of authors [27] in the inverse heat convection problem for
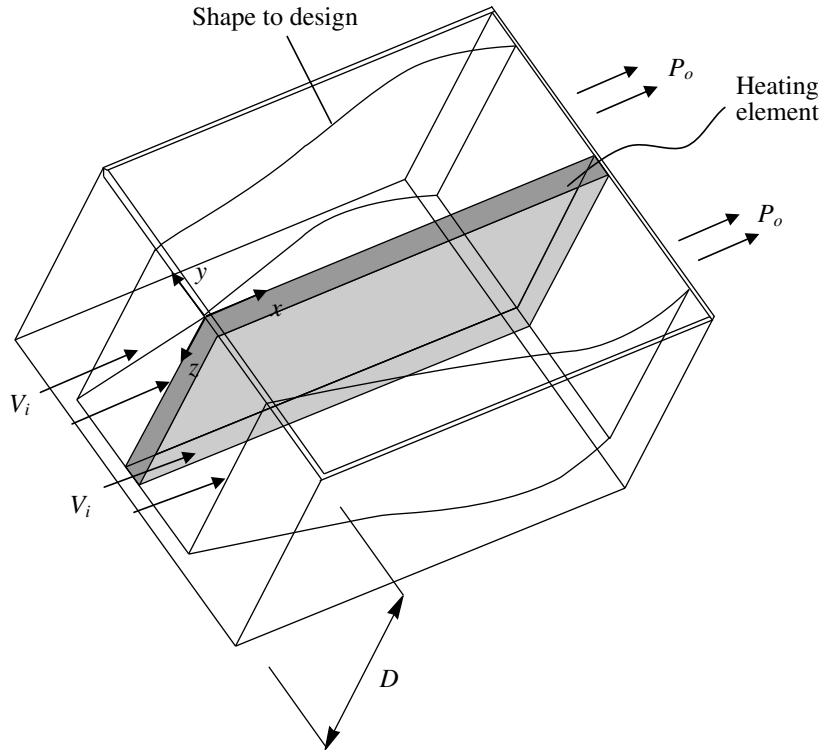
Fig. 1. A millimeter-scale air heater with two symmetric heating channels.

the shape design of a cylinder with uniform temperature distribution on the outer surface.

Fig. 1 shows a millimeter-scale air heater with two symmetric heating channels. Each channel is of width h and length L. Air flow enters the channels at a low temperature T_L and with a uniform velocity of V_i. The inlet and outlet pressures are denoted by P_i and P_o, respectively. Placed in between the two channels is a heating element. In practices, electric heating or heat transfer oil at a high temperature (T_H) can be utilized as the heat source for the heating element. When the aspect ratio of the channels, L/h, is small, a nearly constant temperature along the surface of the heating element can be ensured. On the opposing wall, thermal insulation is used to form an adiabatic boundary to prevent heat loss. The channel width h is a function of x and is denoted by $h(x)$. Note that $h(x)$ is treated as the channel shape function for the adiabatic wall which is to be designed in this study to minimize the objective function. The objective function must be defined in terms of the pressure drop and the heat transfer rate as well so that the channel shape can be designed to fulfill the design purpose.

In this study, a method based on a point-by-point technique for constructing the shape profile is employed. This method is used to determine the irregular profiles that cannot be approximated by the polynomial functions. The relative performance of the point-by-point approach is demonstrated by a comparison with the polynomial function method, and a number of test cases at various inlet velocities are taken into consideration by the former.

2. Theoretical analysis and optimization methods

2.1. Direct problem solver

As the channel depth (D) is relatively large, the analysis is simplified to be a two-dimensional problem. The schematic of the heating channel is shown in Fig. 2. The air is regarded as a Newtonian fluid, and the fluid properties are assumed constant. In addition, within the millimeter-scale channel, the flow field is considered to be steady-state, incompressible, and laminar. Meanwhile, the effects of thermal radiation and buoyancy are neglected. For the air flows, laws of conservation in mass, momentum, and energy can be expressed by the following governing equations:

Mass : $\quad \nabla \cdot \vec{V} = 0$ (1)

Momentum in x-direction : $\quad \rho\left(u\dfrac{\partial u}{\partial x} + v\dfrac{\partial u}{\partial y}\right)$

$$= -\frac{\partial P}{\partial x} + \nabla \cdot (\mu \nabla u) \quad (2)$$

Momentum in y-direction : $\quad \rho\left(u\dfrac{\partial v}{\partial x} + v\dfrac{\partial v}{\partial y}\right)$

$$= -\frac{\partial P}{\partial y} + \nabla \cdot (\mu \nabla v) \quad (3)$$

Energy : $\quad \rho C_P\left(u\dfrac{\partial T}{\partial x} + v\dfrac{\partial T}{\partial y}\right) = \nabla \cdot (k \nabla T) \quad (4)$
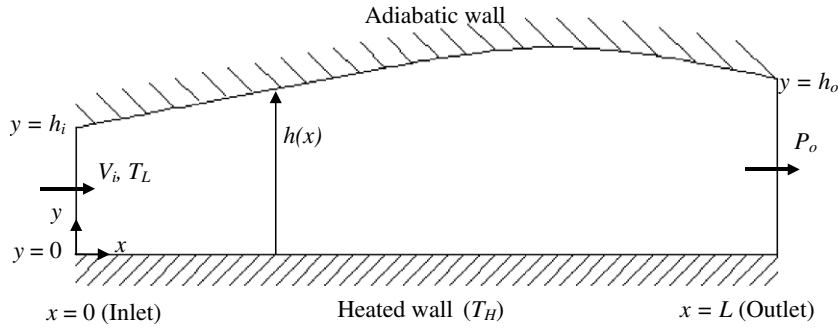
Fig. 2. Schematic of the heating channel.

where the velocity vector and the gradient operator are represented by $\vec{V} = u\vec{i} + v\vec{j}$ and $\nabla \equiv \vec{i}\frac{\partial}{\partial x} + \vec{j}\frac{\partial}{\partial y}$, respectively. The boundary conditions associated with the above governing equations are:

$$u = V_i, \quad v = 0, \quad \text{and} \quad T = T_L \quad \text{at } x = 0 \tag{5a}$$

$$P = P_o \quad \text{and} \quad \frac{\partial T}{\partial x} = 0 \quad \text{at } x = L \tag{5b}$$

$$\vec{V} = 0 \quad \text{and} \quad T = T_H \quad \text{at } y = 0 \tag{5c}$$

$$\vec{V} = 0 \quad \text{and} \quad \frac{\partial T}{\partial N} = 0 \quad \text{at } y = h(x) \tag{5d}$$

where N is the outward normal coordinate to the adiabatic wall at $y = h(x)$.

The above governing equations along with the boundary conditions are solved by adopting the well-accepted finite-element method. In this study, some physical and geometrical variables are fixed. For example, the channel length and the inlet width of the channel are fixed at 10 mm and 1.8 mm, respectively. In addition, the low and high temperatures (T_L and T_H) are fixed at 298 and 328 K. In addition, the thermal properties of air used in the computation are given in Ref. [28], which are provided in the nomenclature. Typically, in each case of simulation the thermal and the flow fields are computed on a mesh having 21×31 structured 4-node two-dimensional cells. Normally, the computation time required to complete an optimization case is approximately 10–12 hours on a personal computer with an AMD-3GHz CPU.

It is important to mention that the emphasis of present study is put on optimization of the millimeter-scale air channel. For doing this, a method based on a point-by-point technique for constructing the shape profile is developed and tested, and is then incorporated with a commonly used optimization algorithm, the SCGM method [26]. To the authors' knowledge, no existing report managed to deal with the millimeter-scale air channel design by using the optimization method. It does not matter whether the direct problem model is simple or complicated. What matters is that the model is practical. For the geometry of the present problem, a two-dimensional model is good enough for numerical predictions. Hence, a more complicated model is not attempted. Besides, in any cases the ideal model must be chosen by considering the balance between accuracy and cost.

2.2. Solver validation

For validation of the direct problem solver, a series of tests were actually conducted, and the comparisons between the present predictions and several existing benchmark solutions had been completed to ensure the adaptability of the code with varying geometry under various velocities. However, to save the space of the paper, not all validation tests are presented and only a typical case directly relevant to the millimeter-scale channel is provided herein. The numerical solutions presented by Olsson et al. [29] for the flow field in a millimeter-scale flat-walled diffuser for a valve-less micropump is compared with the solutions of the present direct problem solver. The results are provided in Fig. 3 to illustrate the validity of the solver. Fig. 3a and b show the solutions provided by Olsson et al. [29] and the present study, respectively. In this case, all the conditions are specified according to the information provided in Ref. [29]. The volumetric flow rate is maintained at 0.0004255 m³/s, and in terms of the definition given in Ref. [29], the corresponding Reynolds number is 460. In addition, the dimensions of the unit are provided in Fig. 3b. The channel is of length 1.093 mm with opening angle of 9.8° and smallest channel width of 0.08 mm. It is found that the comparison shows close agreement between the two sets of data. The maximum velocity is predicted to be 6.067 m/s at the inlet with smallest width, which is exactly equal to the value given in Fig. 3a. Meanwhile, the small asymmetry at the outlet, which could be caused by the asymmetric upstream conditions and was found by the authors, is also observed in the present solution.
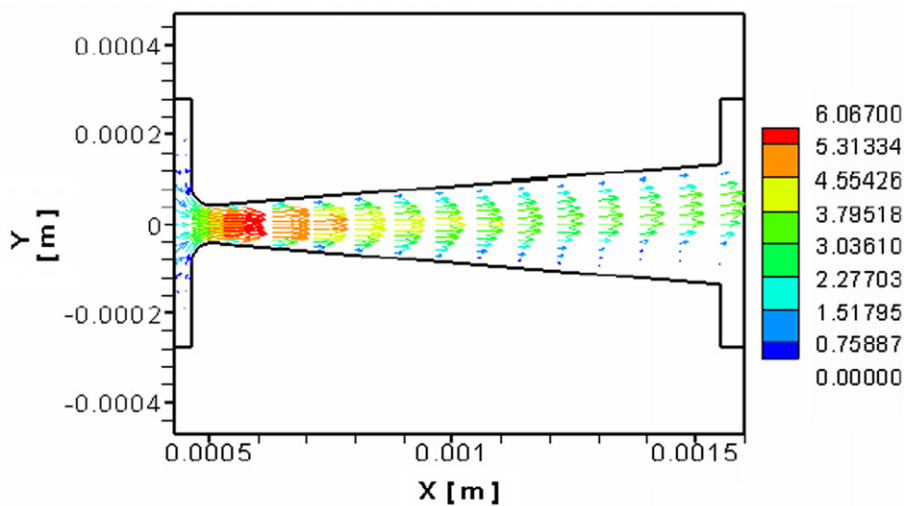
2.3. Optimization method

In the present study, an objective function (J) in conjunction with the optimization process leading to the desired channel shape is defined in the following:

$$J = \frac{1}{C_1 \left[\frac{C_p (T_o - T_i)}{L_s} \right] + C_2 \left[\frac{L_s}{P_i - P_o} \right]} \tag{6}$$
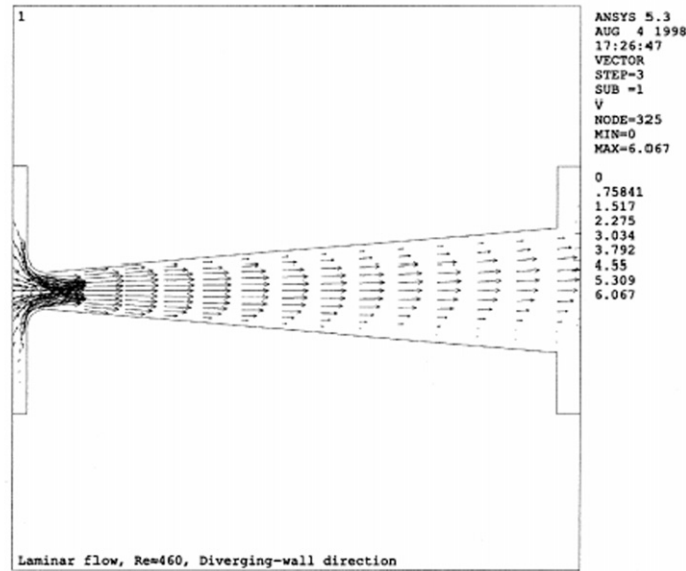
(a) Olsson, Stemme, and Stemme [29]

(b) Present

Fig. 3. Comparison of the predictions of flow field in a millimeter-scale flat-walled diffuser by the present solver with existing report [29].

where the first term in the braces on the right-hand side of the equation represents the magnitude of the average heat flux transferred to the air, and the second term represents the magnitude of the average pressure gradient. The objective function is expressed by taking the reciprocal of the summation of these two terms, and the values of C_1 and C_2 are the weighting constants which are specified by the users arbitrarily based on the requirement of the design purpose. In this manner, as the objective function J is approaching its minimum value in the optimization process, with the definition of J, the average heat flux gradually reaches a maximum while the average pressure gradient is being reduced to a minimum. This implies that a lower pressure drop accompanied by a higher heat transfer can be obtained. The process of weighting involves emphasizing one of the two aspects, heat transfer or pres-

sure drop. For example, in a case that the reduction of the pressure drop is emphasized, one lets $C_1 \ll C_2$. On the contrary, when the heat transfer performance is desired, one may have $C_1 \sim C_2$. In the present study, typically the value of C_1 is assigned to be 1.0 and C_2 is 200.

Let $\{a_i | i = 1, 2, \ldots, k\}$ be the set of the undetermined coefficients to be optimized in the iterative process. Different combinations of these coefficients represent different shape profiles among which the optimal shape may be found. In other words, in the optimization process, the coefficients $\{a_i | i = 1, 2, \ldots, k\}$ are updated iteratively toward the minimization of the object function.

The minimization of the objective function is accomplished by using the SCGM method [26]. The method evaluates the gradient functions of the objective function and sets up a new conjugate direction for the updated

undetermined coefficients with the help of a direct numerical sensitivity analysis [26]. The procedure for applying the SCGM method is described briefly in the following:

(1) Make an initial guess for the shape profile by giving initial values to the set of undetermined coefficients $\{a_i | i = 1, 2, \ldots, k\}$.
(2) Use the direct problem solver to predict the thermal and flow fields associated with the latest shape profile, and calculate the objective function J by Eq. (6).
(3) When the objective function reaches a minimum, the solution process is terminated. Otherwise, proceed to step (4).
(4) Perform the direct numerical sensitivity analysis [26] to determine the gradient functions $(\partial J / \partial a_i)^n (i = 1, 2, \ldots, k)$. First, give a perturbation (Δa_i) to each of the undetermined coefficients $\{a_i | i = 1, 2, \ldots, k\}$, and then find the change in the objective function (ΔJ) caused by Δa_i. Then, the gradient function with respect to each of the undetermined coefficients $\{a_i | i = 1, 2, \ldots, k\}$ can be calculated by the direct numerical differentiation as

$$\frac{\partial J}{\partial a_i} = \frac{\Delta J}{\Delta a_i} \qquad (7)$$

(5) Calculate the conjugate gradient coefficients γ_i^n and the search directions π_i^{n+1} for each of the undetermined coefficients $\{a_i | i = 1, 2, \ldots, k\}$ with

$$\gamma_i^n = \left[\frac{\left(\frac{\partial J}{\partial a_i}\right)^n}{\left(\frac{\partial J}{\partial a_i}\right)^{n-1}} \right]^2, \quad i = 1, 2, \ldots, k \qquad (8)$$

$$\pi_i^{n+1} = \left(\frac{\partial J}{\partial a_i}\right)^n + \gamma_i^n \pi_i^n, \quad i = 1, 2, \ldots, k \qquad (9)$$

(6) Assign a fixed value to the step sizes $\beta_i (i = 1, 2, \ldots, k)$ for all the undetermined coefficients $\{a_i | i = 1, 2, \ldots, k\}$ and leave it unchanged during the iteration. In this study, the fixed value is determined by a trial- and error process, and the value is set to be 1.0×10^{-6} typically.
(7) Update the undetermined coefficients and hence the shape profile with

$$a_i^{n+1} = a_i^n - \beta_i \pi_i^{n+1}, \quad i = 1, 2, \ldots, k \qquad (10)$$

and then go back to step (2).

2.4. Description of shape profiles

The shape profile of the channel could be built by using a polynomial function. However, not all shape profiles can be approximated by the polynomial function. If the shape profile is irregular and cannot be cast into a polynomial function accurately, there must exist a remarkable error in the predictions. Thus, the flexibility of the method using the polynomial function is actually limited. In the present study, the shape profile is built by using a point-by-point approach which uses no mathematical expression for the channel shape. Therefore, this approach is particularly suitable for the design of the irregular shape profile. In the following, a number of test cases are taken into consideration to demonstrate the validity of the present point-by-point approach. For comparison, both the polynomial function and the point-by-point approaches are applied to evaluate the relative performance of the present approach.

2.5. Polynomial function approach

In this study, two polynomial functions are in use. The first one is a linear polynomial function. That is

Shape function 1: $\quad h(x) = b_1 + b_2 x \qquad (11)$

Note that in general the channel shape profile cannot be as simple as a linear function. The reason for using Eq. (11) is simply for comparison. The second function is a polynomial function of degree 3:

Shape function 2: $\quad h(x) = c_1 + c_2 x + c_3 x^2 + c_4 x^3 \qquad (12)$

When shape function 1 is applied, the coefficients b_1 and b_2 are regarded as the undetermined coefficients to be optimized in the iterative process. Similarly, when shape function 2 is applied, the undetermined coefficients are just the coefficients c_1, c_2, c_3, and c_4.

2.6. Point-by-point approach

In the point-by-point approach, the shape profile is not defined by any mathematical expression but a series of values of the channel width at different locations along the streamwise direction. The channel width at $x = x_i$ is denoted by $h_i (i = 1, 2, \ldots, k)$. The set of the channel widths at all the streamwise points are regarded as the designed variables to optimize. Since in this study there are 21 cells in the x-direction on the mesh in use, the number of the designed variables (k) is 21. The values of h_i at all the points are then used to plot the shape profile in a piecewise manner. Note that a smoother profile can be obtained as more points are taken into consideration. However, a larger number of the points means a larger group of the cells and the undetermined coefficients. The number of the points was chosen by considering a balance between shape profile quality and computation cost.

In the following, a group of test cases are taken into consideration to demonstrate the validity of the present point-by-point approach. For the test cases, shape designs are carried out based on the polynomial function and the point-by-point approaches to display the relative performance of the latter.

3. Results and discussion

Fig. 4 shows the results of channel shape design by using the two approaches for the case at $V_i = 0.15$ m/s. At this velocity, the Reynolds number ($Re = \rho V_i h_i / \mu$) is equal to

17.94. The initial guess for the channel shape is set by a parallel-plate channel [$h(x) = h_i$] for each case. In general, starting from the initial guess, it required approximately 100 iterations to reach the optimal shape. In this figure, the optimal shapes obtained by shape functions 1 and 2 are plotted with the dash-dotted and the dotted curves, respectively. However, just because the polynomial function approach has the convergent solutions does not mean it is correct. It is clearly found that the outcome of the polynomial function method is limited by the function form. In short, shape function 1 can only lead to a linear divergent channel (with a 6.26-mm outlet height), and shape function 2 to an optimal shape profile that can be portrayed by a polynomial function of degree 3 (with $c_1 = 1.8 \times 10^{-3}$, $c_2 = 0.7332$, $c_3 = -5.3823$, and $c_4 = -1506.136$). The polynomial function approach fails to provide accurate predictions for an irregular channel.

On the other hand, the advantages of the point-by-point approach can be clearly observed. The optimal shape profile obtained by the point-by-point approach is plotted by the solid curve in Fig. 4. The optimal channel features a similar pattern of a divergent diffuser; however, it is seen that this approach provides an irregular optimal shape profile of the channel that definitely cannot result from the polynomial function method. Furthermore, the minimum values of the objective function reached by shape functions 1 and 2 are 3.259×10^{-3} and 3.112×10^{-3}, respectively, while by the point-by-point approach the minimum objective function is reduced to 2.836×10^{-3}. This implies that the point-by-point approach is really able to portray the irregular shape more accurately. Therefore, the approach is suitable to be incorporated with the SCGM method to pursue the optimal shape of the channel. Fig. 5 displays the velocity, temperature, and pressure distributions in the channel with optimal shape obtained by the point-by-

point method, at $V_i = 0.15$ m/s. The numerical predictions of the thermal and flow fields associated with the irregular shape profile is carried out by using the direct problem solver. It is noticed that low pressure regions are present near the top wall at the inlet signifying possible presence of vortex structures.

The value of objective function varying in iteration is shown in Fig. 6 for the same case. It is observed that the objective functions is slightly increased in the first 60 iterations, and then is decreased rather rapidly. At the 114th iteration, the minimum value of 2.836×10^{-3} is reached. In this figure, the initial guess, the optimal shape profile, and the iterative shape profiles at 40th and 80th iterations are also provided. It can be found in this figure that the iterative shape profile experiences a greater variation in the process and eventually attains convergence.

The optimal shapes at different inlet velocities are investigated. The inlet velocity (V_i) is one of the major influential parameters affecting the heat transfer behavior and pressure drop in the channel. Therefore, to study the effects of the inlet velocity, the approach has been applied to

(a) Velocity vector plot

(b) Temperature distribution

(c) Pressure distribution

Fig. 5. Velocity, temperature, and pressure distributions in the channel with optimal shape obtained by the point-by-point method, at $V_i = 0.15$ m/s. (a) Velocity vector plot, (b) temperature distribution, and (c) pressure distribution.
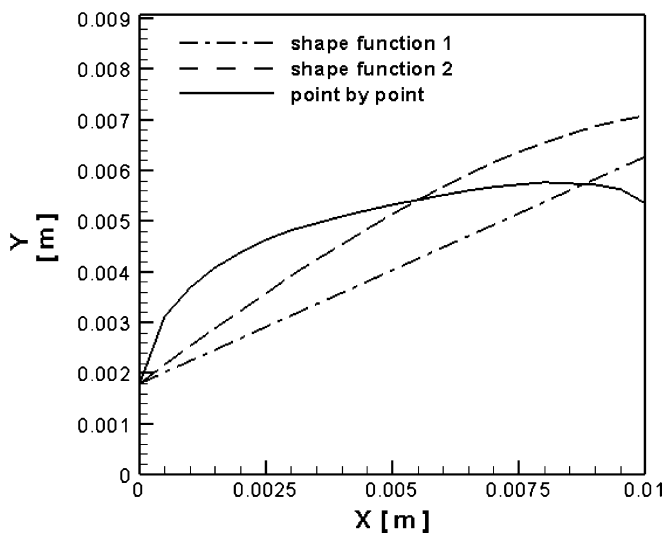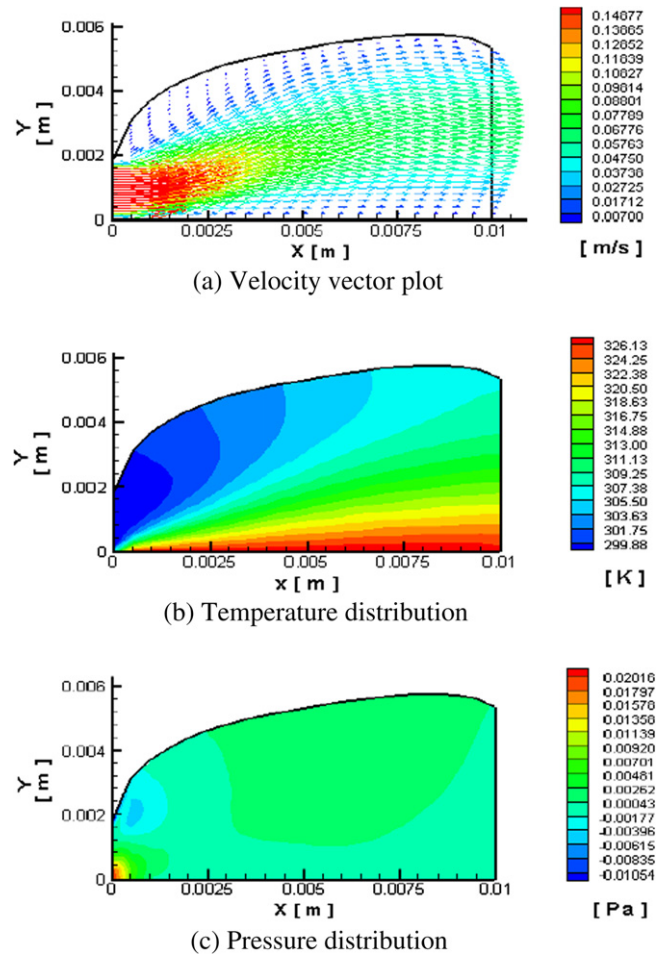

Fig. 4. Comparison in optimal design for channel shape between polynomial-function and the present point-by-point approaches, for case at $V_i = 0.15$ m/s.
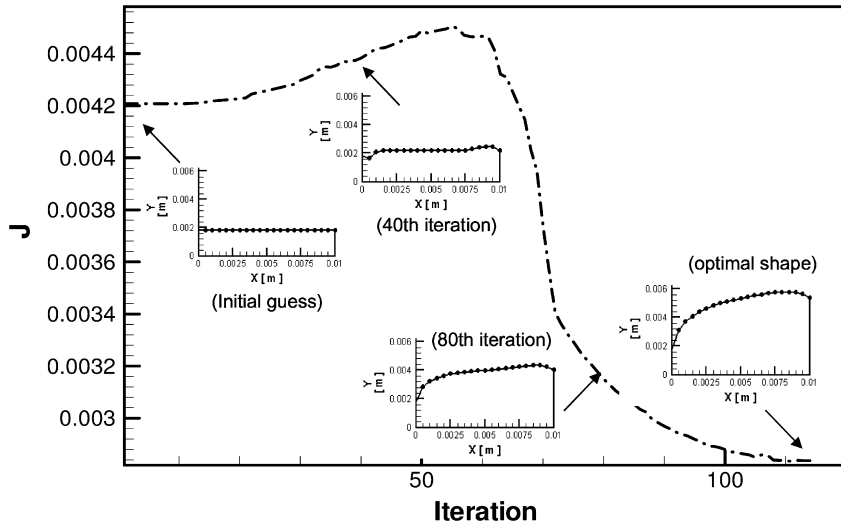
Fig. 6. Variation of objective function in iteration, for the case at $V_i = 0.15$ m/s.

design the channel shape profile at different inlet velocities, and Fig. 7 shows part of the results. In this figure, the optimal shape profiles at $V_i = 0.1$ and 0.15 m/s are plotted. Based on the results shown in Fig. 7, it is found that the channel design indeed exhibits great dependence on the inlet velocity. The optimization process leads to a wider channel at $V_i = 0.1$ m/s than at $V_i = 0.15$ m/s. The information regarding the inlet and the outlet conditions of the optimal designs is provided in a table given in this figure. It is seen that using the optimization method the average outlet temperatures of the air at $V_i = 0.1$ m/s can be elevated to a value (314.345 K) very close to that of the optimal case at $V_i = 0.15$ m/s (314.368 K). At the same time, the average pressure drop between the inlet and the outlet ($P_i - P_o$) is reduced to 7.796×10^{-3} Pa for the case at $V_i = 0.1$ m/s, which is lower than the pressure drop at $V_i = 0.15$ m/s, 8.108×10^{-3} Pa.
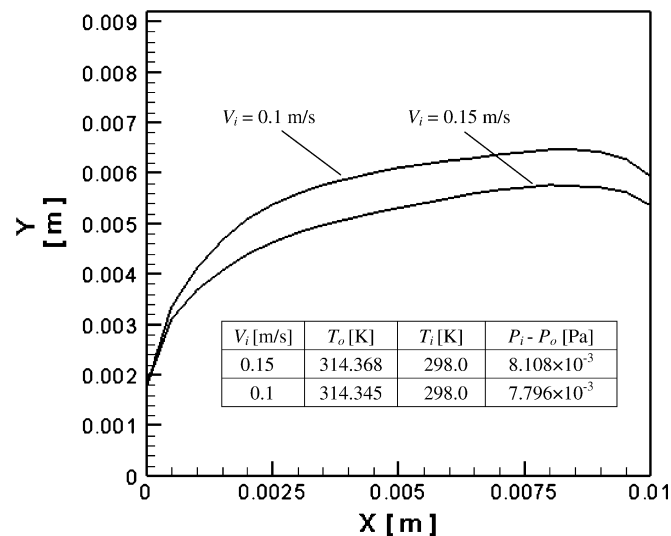
Note that the initial guess for the channel shape can be given arbitrarily in a certain extent. One may have reasons to suspect that the point-by-point method might not lead to unique solution when different initial guesses are used. To test the uniqueness of the predictions, in addition to the case using the parallel-plate channel as the initial guess, two other initial guesses are adopted: one is a linear divergent channel; and the other is a linear convergent channel. Fig. 8 shows the iterative shape profiles in the optimization processes based on these two different initial guesses. Results of the case using the linear divergent channel are plotted in the left portion, and those of the case using the linear convergent channel in the right. In a comparison between the two cases, it is interesting to find that even though the tentative shape profiles are quite different, the optimal solutions of the two cases are in close agreement regardless of the initial guesses. In addition, both the two solutions are identical to the optimal shape profile yielded by using the parallel-plate channel as the initial guess shown in Fig. 6. It is also noted that the numbers of iterations required to reach the optimal designs for the linear divergent, parallel-plate, and linear convergent channels are 106, 114, and 130, respectively. The pattern of the linear divergent channel is essentially closer to that of the optimal channel shape; therefore, this case attains faster convergence than the other two cases.

Performance of the optimized channel may be demonstrated by numerical simulation in a direct comparison to the traditional parallel-plate and the divergent channels. For making a fair assessment, the arithmetic average of the width of the optimized channel ($\bar{h}$) is first calculated. The result is $\bar{h} = 4.917$ mm for the case at $V_i = 0.15$ m/s. The width of the compared parallel-plate channel is then set to be 4.917 mm and the inlet velocity is also assigned to be 0.15 m/s. In this study, both the inlet velocity and the inlet width are fixed, and hence the mass flow rate is kept constant. The relative magnitude of average heat flux

V_i [m/s]	T_o [K]	T_i [K]	P_i - P_o [Pa]
0.15	314.368	298.0	8.108×10⁻³
0.1	314.345	298.0	7.796×10⁻³

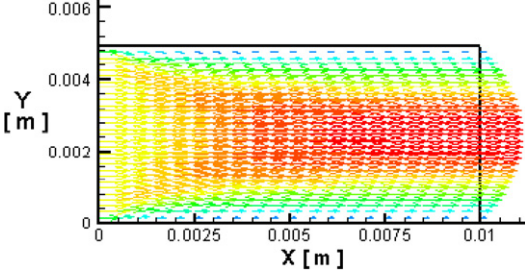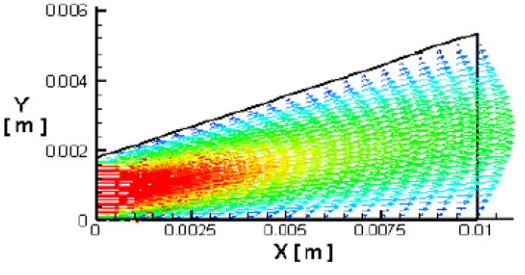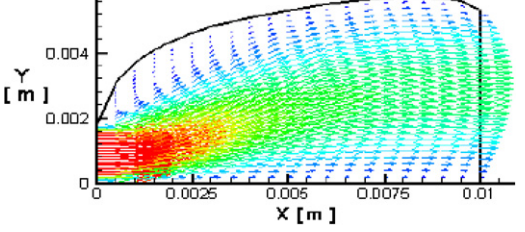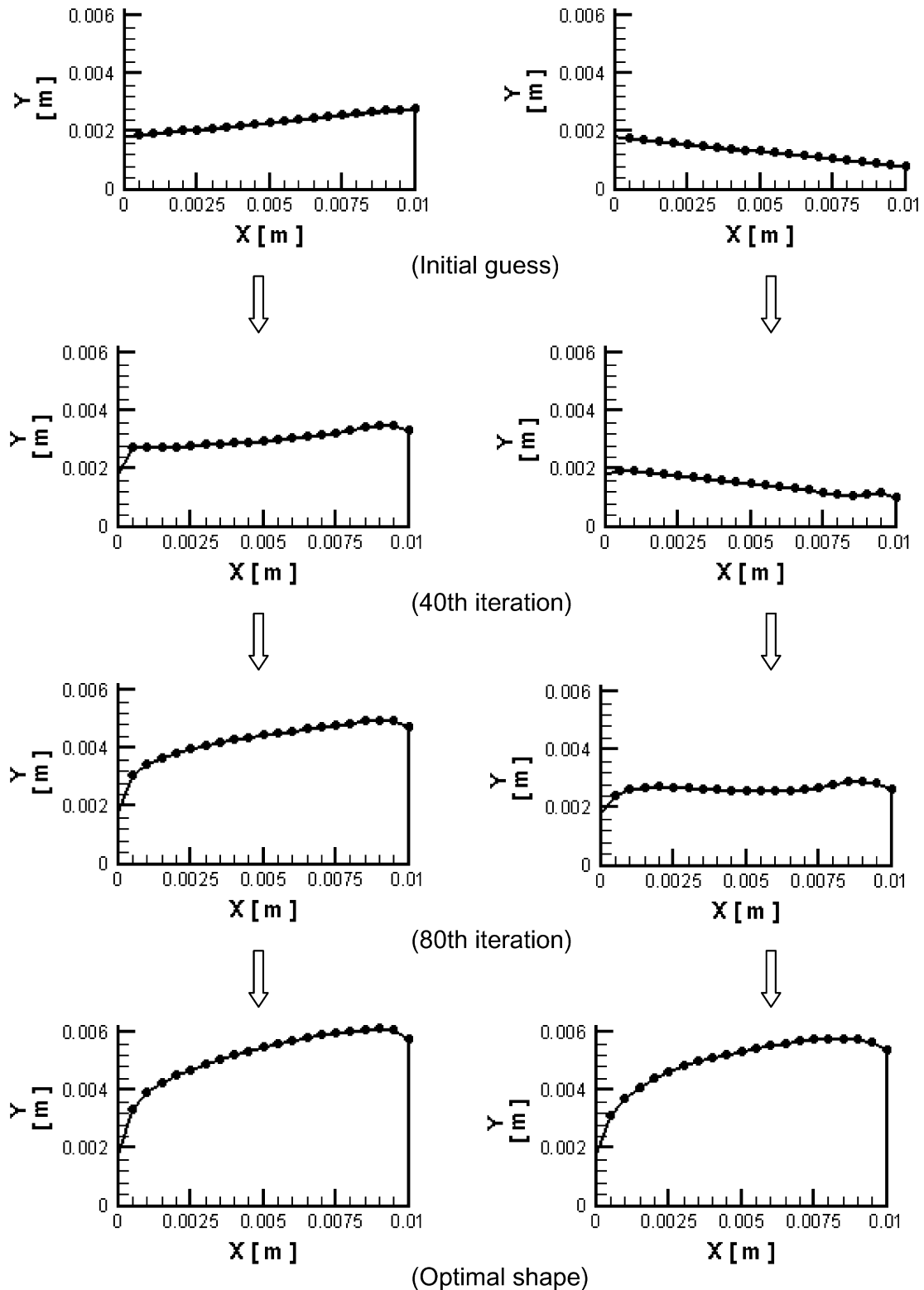Fig. 7. Effects of the inlet velocity on the optimal channel shape.

Fig. 8. Iterative shape profiles in the optimization process based on different initial guesses, for the case at $V_i = 0.15$ m/s.

transferred to the air can then be compared simply based on the data of temperature rise. According to the results shown in Table 1, it is found that the optimized channel exhibits much higher performance than the parallel channel. As seen in this table, the temperature rise of the fluid

flowing through the parallel-plate is only 8.325 K at a pressure drop of 2.315×10^{-2} Pa. In the optimized channel, the fluid temperature can be increased by 16.368 K, and the pressure drop can be reduced to be 8.108×10^{-3} Pa. In addition, the data associated with the divergent channel

Table 1
Performance of the optimal design for $V_i = 0.15$ m/s

Channel	$T_o - T_i$ (K)	$P_i - P_o$ (Pa)	Flow field
Parallel-plate channel with $h(x) = 4.917$ mm	8.325	2.315×10^{-2}	
Divergent channel of the same inlet and outlet widths as the optimal channel	16.9265	1.448×10^{-2}	
Present optimal channel	16.368	8.108×10^{-3}	

of the same inlet and outlet widths as the optimal channel are also provided in this table. A comparison between the divergent and the optimal channels shows that they have nearly equal temperature rises; however, the pressure drop of the optimal channel is much lower than that of the divergent channel, 1.448×10^{-2} Pa. Therefore, the relative performance of the optimal channel is observed. The shape

profile of the channel can be optimized to meet the design purpose by using the present optimization approach. It is noticed that the pressure drop includes the reversible pressure head increase due to area change. As a matter of fact, the direct problem solver will automatically take into account both the friction and the area-changing effects in the optimization process.

Fig. 9 shows the dependence of optimal shape on the value of C_2 at $C_1 = 1.0$. It is found that if the value of C_1 is fixed, the value of C_2 can affect the resulting optimal shape of the channel; however, the dependence of the optimal design on C_2 is rather insensitive. As already stated earlier, the specification is open to the users depending on the requirement of the design purpose.
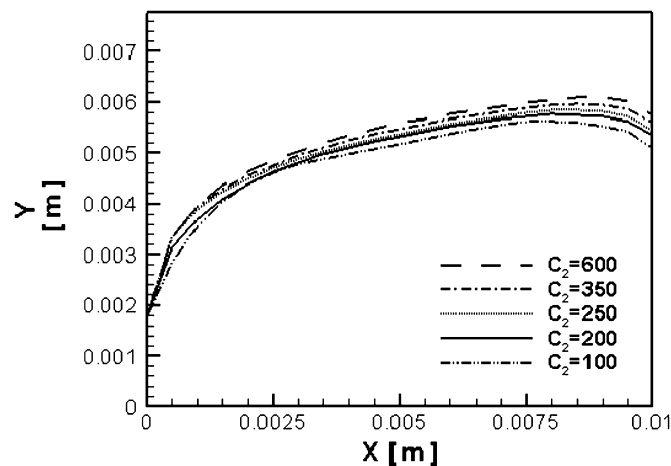
4. Concluding remarks

Shape design of a millimeter-scale air channel for increasing heat transfer and reducing pressure drop is performed. The numerical design approach is developed by combining a direct problem solver with an optimization method. A two-dimensional theoretical model is used to develop the direct problem solver for predicting the thermal and flow fields associated with the varying shape profile during the iterative optimization process. On the other

Fig. 9. Dependence of optimal shape on the value of C_2 at $C_1 = 1.0$.

hand, the simplified conjugate gradient method (SCGM) [26] is used as the optimization method to minimize the objective function expressed in terms of the average pressure drop and the average heat flux.

In this study, a method based on a point-by-point technique for constructing the shape profile is incorporated with the SCGM method to pursue the optimal shape of the channel. It is observed that the point-by-point approach is really able to portray the irregular shape more accurately, as compared with the polynomial function approach.

In addition, the optimal shapes at different inlet velocities are investigated, and the optimal shape profiles at $V_i = 0.1$ and 0.15 m/s are plotted. Results show that the channel design indeed exhibits great dependence on the inlet velocity. The optimization process leads to a wider channel for the case at $V_i = 0.1$ m/s than at $V_i = 0.15$ m/s. It is also seen that using the optimization method the average outlet temperatures of the air at $V_i = 0.1$ m/s can be elevated to a value very close to that of the optimal case at $V_i = 0.15$ m/s. At the same time, the average pressure drop between the inlet and the outlet ($P_i - P_o$) is reduced to 7.796×10^{-3} Pa for the case at $V_i = 0.1$ m/s, which is lower than the pressure drop at $V_i = 0.15$ m/s, 8.108×10^{-3} Pa.

To test the uniqueness of the predictions, three different initial guesses for the channel shape profile are used, namely, parallel-plate channel, linear divergent channel and linear convergent channel. It is interesting to find that even though the tentative shape profiles are quite different, the optimal solutions of the three cases are in close agreement regardless of the initial guesses.

The performance of the optimized channel has been demonstrated by numerical simulation in a direct comparison to the traditional parallel-plate and the divergent channels. Results show that the optimal shape profile of the yielded by the present optimization approach channel meets the design purpose.

References

[1] N.V. Shumakov, A method for the experimental study of the process of heating a solid body, Soviet Phys.–Tech. Phys. 2 (1957) 771, Translated by American Institute of Physics.

[2] G. Stolz Jr., Numerical solutions to an inverse problem of heat conduction for simple shape, J. Heat Transfer 82 (1960) 20–26.

[3] C.H. Huang, C.W. Chen, A boundary-element-based inverse problem of estimating boundary conditions in an irregular domain with statistical analysis, Numer. Heat Transfer, Part B 33 (1998) 251–268.

[4] M. Prud'homme, T.H. Nguyen, On the iterative regularization of inverse heat conduction problems by conjugate gradient method, Int. Comm. Heat Mass Transfer 25 (1998) 999–1008.

[5] C.H. Huang, S.P. Wang, A three-dimensional inverse heat conduction problem in estimating surface heat flux by conjugate gradient method, Int. J. Heat Mass Transfer 42 (1999) 3387–3403.

[6] H.M. Park, O.Y. Chung, An inverse natural convection problem of estimating the strength of a heat source, Int. J. Heat Mass Transfer 42 (1999) 4259–4273.

[7] C.H. Huang, M.N. Ozisik, B. Sawaf, Conjugate gradient method for determining unknown conduct conductance during metal casting, Int. J. Heat Mass Transfer 35 (1992) 1779–1786.

[8] P. Terrola, A method to determine the thermal conductivity from measured temperature profiles, Int. J. Heat Mass Transfer 32 (1989) 1425–1430.

[9] T.P. Lin, Inverse heat conduction problem of simultaneously determining thermal conductivity, heat capacity and heat transfer coefficient, Master Thesis, Department of Mechanical Engineering, Tatung Institute of Technology, Taipei, Taiwan, 1998.

[10] H.H. Lin, C.H. Cheng, C.Y. Soong, F.L. Chen, W.M. Yan, Optimization of key parameters in proton exchange membrane fuel cell, J. Power Sources 162 (2006) 246–254.

[11] C.H. Cheng, H.H. Lin, G.J. Lai, Design for geometric parameters of PEM fuel cell by integrating computational fluid dynamics code with optimization method, J. Power Sources 165 (2007) 803–813.

[12] G. Fabbri, Optimum profiles for asymmetrical longitudinal fins in cylindrical ducts, Int. J. Heat Mass Transfer 42 (1999) 511–523.

[13] G. Fabbri, Heat transfer optimization in corrugated wall channels, Int. J. Heat Mass Transfer 43 (2000) 4299–4310.

[14] C.H. Cheng, M.H. Chang, Design of irregular slider surface for satisfying specified load demands, ASME J. Mech. Des. 127 (2005) 1184–1185.

[15] K. Park, D.H. Choi, K.S. Lee, Numerical shape optimization for high performance of a heat sink with pin-fins, Numer. Heat Transfer, Part A 46 (2004) 909–927.

[16] W. Gao, P.D. Hodgson, L. Kong, Numerical analysis of heat transfer and the optimization of regenerators, Numer. Heat Transfer, Part A 50 (2006) 63–78.

[17] K.Y. Kim, Y.M. Lee, Design optimization of internal cooling passage with V-shaped ribs, Numer. Heat Transfer, Part A 51 (2007) 1103–1118.

[18] C.H. Cheng, M.H. Chang, Identification of unknown geometry and temperature for heating elements embedded in a rectangular package, ASME J. Heat Transfer 127 (2005) 918–930.

[19] J.S. Maeng, S.Y. Han, Application of the growth-strain method for shape optimization of flow systems, Numer. Heat Transfer, Part A 45 (2004) 235–246.

[20] E. Divo, A.J. Kassab, F. Rodriguez, An efficient singular superposition technique for cavity detection and shape optimization, Numer. Heat Transfer, Part B 46 (2004) 1–30.

[21] S.H. Ha, S. Cho, Topological shape optimization of heat conduction problems using level set approach, Numer. Heat Transfer, Part B 48 (2005) 67–88.

[22] E. Nobile, F. Pinto, G. Rizzetto, Geometric parameterization and multiobjective shape optimization of convection periodic channels, Numer. Heat Transfer, Part B 50 (2006) 425–453.

[23] M.W. Wambsganss, J.A. Jendrzejczyk, D.M. France, Two-phase flow and pressure drop in flow passages of compact heat exchangers, in: 1992 SAE International Congress and Exposition, February 24–28, Detroit, MI, USA, 1992.

[24] L.A. Campbell, S. Kandlikar, Experimental study of heat transfer, pressure drop, and dryout for flow boiling of water in an oil heated minichannel, in: Proceedings of the 2nd International Conference on Microchannels and Minichannels, June 17–19, Rochester, New York, USA, 2004.

[25] M. Bahrami, M.M. Yovanovich, Pressure drop of fully-developed, laminar flow in microchannels of arbitrary cross-section, ASME J. Fluids Eng. 128 (2006) 1036–1044.

[26] C.H. Cheng, M.H. Chang, A simplified conjugate-gradient method for shape identification based on thermal data, Numer. Heat Transfer, Part B 43 (2003) 489–507.

[27] C.H. Cheng, M.H. Chang, Shape design for a cylinder with uniform temperature distribution on the outer surface by inverse heat transfer method, Int. J. Heat Mass Transfer 46 (2003) 101–111.

[28] S. Kakac, R.K. Shah, W. Aung, Handbook of Single-phase Convective Heat Transfer, Wiley, New York, 1987.

[29] A. Olsson, G. Stemme, E. Stemme, Numerical and experimental studies of flat-walled diffuser elements for valve-less micropump, Sensors Actuators 84 (2000) 165–175.